A New Tracing Algorithm for Automatic Boundary Extraction from Coronary Cineangiograms

Farsad Zamani Boroujeni, Rahmita Wirza, Norwati Mustapha,Lilly Suriani Affendey,
Oteh Maskon and Majid Khalilian

***Abstract*— The need for reliable identification of vessel contours from X-ray image sequences within a limited computation time is still a challenge in medical image analysis. In the literature, only a few vessel boundary extraction methods are suitable to meet automatic and real-time constraints for capturing and processing coronary artery cineangiograms. Among many approaches, vessel tracing algorithms are known to be fast and robust for practically detecting the vessel structures from live two- dimensional angiogram sequences. However, they often do not directly extract the boundary points and instead the locations of boundary points are achieved after identifying the correct position of centerline points. This boundary detection scheme seems to be less efficient in speed demanding clinical applications. In this paper a new algorithm for automatic tracing of vessel boundaries using an efficient estimation of local gradient vector is presented. The results illustrate that our method is a promising method for real-time vessel segmentation and linear feature extraction.**

***Index Terms*—Feature extraction, real-time systems, segmentation, tracing, tracking.**

I. INTRODUCTION

Real-time linear feature extraction is broadly utilized as a fundamental underlying task in most kinds of real-time image processing systems. Generally, there are two schemes described in the literature for extracting linear structures from 2D images: 1) segmenting a complete network of vessel structure; and 2) directly explore the boundaries or centerlines using an exploratory tracing algorithm. The first scheme consists of a wide range of segmentation techniques such as filtering and edge operator techniques [1], pixel classification techniques [2], mathematical morphology approaches [3], wave propagation techniques [4], flux maximizing geometric approach [5] and many others.

In these techniques the primary goal is to identify the pixels located on the specific areas of the image covered by the structures of interest. They require extensive processing of image pixels and generally rely on adaptive segmentation, followed by extracting boundaries, centerlines and branch point analysis. Even though they give accurate results, they require much time and computational resources to complete the task.

The second approach, employed by this paper and several others [6]-[11], is referred to as vectorial tracing or vessel tracing. These methods usually avoid low level preprocessing steps and instead, locate a number of initial seed points by a spatially sparse search over the image and only process the pixels which are close to the feature of interest. These approaches often rely on automatic detection of seed points which are assumed to be located on the centerline of the vessels [8]-[11]. Since some of the detected seed points may correspond to noise, the tracing algorithm must verify the existence of the local vessel borders in the small neighborhood around the seed point. However, this verification increases the computational load and is unnecessary for tracing the vessel boundaries in the image.

The method presented in this paper focuses on directly detecting the valid boundary points and merely tracing single boundaries along the direction vector perpendicular to the local gradient vector. It has resulted in the adaptation, after appropriate refinements, of the technique proposed by Can et al. [8] which has been developed for feature extraction from retinal fundus images. Our tracing algorithm is very fast and exhibits desirable results when applied to live X-ray image sequences.

II. METHOD

The following outline presents an overview of the processes involved in our tracing algorithm:

1) Collecting a number of initial points (seed points) by exploring the image along a grid of 1 pixel-wide lines using one-dimensional edge detection kernel.
2) Applying a set of verification rules and examining the local geometric properties of gradient vectors correspond to each seed point to test the validity of the seed point.
3) Starting a new exploratory search initiated at each of the validated seed points and calculating the location of the next boundary point in a recursive manner.
4) Refining the location of the next point calculated in step3 in order to obtain smoother traces.

Our tracing algorithm is applied to digital X-ray coronary angiograms. For this reason, some assumptions should be made before discussing the details of our algorithm.

Manuscript received October 2, 2009.

Farsad Zamani Boroujeni is a faculty member in Islamic Azad University, Khorasgan Branch, Esfahan, Iran and Ph.D student in computer science, Faculty of Computer Science and Information Technology, Universiti Putra Malaysia, Malaysia. (e-mail: farsad.zamani@ ieee.org).

Rahmita Wirza, Norwati Mustapha and Lilly Suriani Affendey are with Faculty of Computer Science and Information Technology, Universiti Putra Malaysia, Malaysia. (e-mails: rahmita@fsktm.upm.edu.my, norwati@ fsktm.upm.edu.my, suriani@ fsktm.upm.edu.my).

Oteh Maskon is with Department of Medicine, Hospital Universiti Kebangsaan Malaysia, Malaysia. (e-mail: auajwad@yahoo.com).

Majid Khalilian is a faculty member in Islamic Azad University, Karaj Branch, Karaj, Iran. (e-mail: khalilian@ieee.org).

ISBN: 978-988-18210-4-1
ISSN: 2078-0958 (Print); ISSN: 2078-0966 (Online)

Typically, different angiograms exhibit variations in brightness, contrast and the presence of imaging artifacts. Nevertheless, it is assumed that the features of interest are darker than the local background. It is also assumed that they have well-defined edges and locally continuous. The changes in direction along the borders are smooth and finally, the images are expected to be corrupted minimally by Gaussian noise.

A. Automatic Collection of Seed Points

Due to possible existence of discontinuities and high curvature in the boundaries, the tracing algorithm would need to be initiated at several seed points. Whenever the trace point reaches to background areas and low contrast edges, the algorithm would stop the current trace and starts a new trace initiated at next seed point and finally the traces are combined. The true seed points are located on the boundaries (edges) of the vessels. For this reason, the seed points are identified using one-dimensional edge detector kernel of the form [1, 2, 0, -2, -1] ^{T} along a set of horizontal and vertical grid lines. By sliding the 1-D kernel, the points with maximum absolute value of the kernel response are identified as the candidate points and are collected for validation in the next step.

B. Seed Point Validation

Ideally, the tracing algorithm must start at the seed points which are located on the vessel boundaries. However, vessels only cover a small portion of the image area and, therefore, a large number of collected points lie on the background and must be discarded.

In the mathematical point of view, the gradient vector is perpendicular to the surface of the level curves. This property can be used for discarding the seed points that have neighbors with different directions. Fig. 1 illustrates a small part of a gradient vector field calculated for a sample vessel structure. This figure depicts the following features of the gradient vectors located inside and near the boundaries of the vessel:

1) The gradient vectors of the points that are located on the same boundary within a small distance have nearly equal directions.
2) The gradient vector of each point and its diametrically opposite point located on the opposite boundary must have nearly opposite directions.

In fact, the validation procedure employs these properties and verifies the symmetric features of the gradient vectors at the neighborhood of the candidate points and their corresponding points located on the opposite edge. For this purpose, two 5x5-gradient masks are used for calculating the x and y gradients at each seed point *P(x,y)*. The horizontal and vertical gradient components ∇_x and ∇_y are given as follows:

$$\nabla_x = \begin{pmatrix} -1 & -2 & 0 & 2 & 1 \\ -1 & -2 & 0 & 2 & 1 \\ -1 & -2 & 0 & 2 & 1 \\ -1 & -2 & 0 & 2 & 1 \\ -1 & -2 & 0 & 2 & 1 \end{pmatrix} \quad \nabla_y = \begin{pmatrix} 1 & 1 & 1 & 1 & 1 \\ 2 & 2 & 2 & 2 & 2 \\ 0 & 0 & 0 & 0 & 0 \\ -2 & -2 & -2 & -2 & -2 \\ -1 & -1 & -1 & -1 & -1 \end{pmatrix} \tag{1}$$

In addition, these estimates can be used for calculating the angle θ_p between the gradient vector $\overrightarrow{\nabla p^i} = [\nabla_x p \ \nabla_y p]^T$ (calculated at point p) and the x-axis:

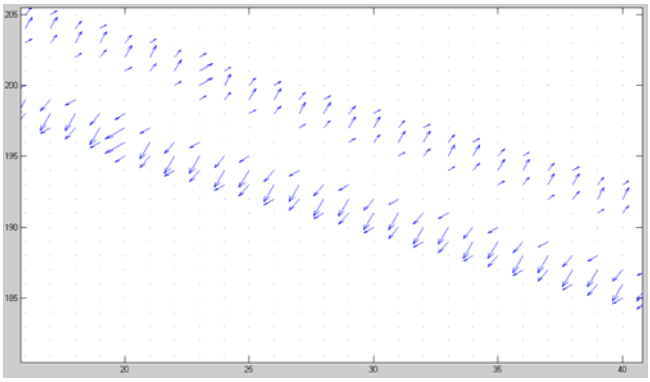

Fig. 1. A gradient vector field for a small part of a vessel structure.

$$\theta_p \cong tan^{-1} \frac{\nabla_y p}{\nabla_x p} \tag{2}$$

In order to avoid expensive calculations for computing trigonometric function, a two-dimensional look-up table data structure is used. By observing the numerical coefficients in (1), for all intensity values in the image, the gradient components ∇_x and ∇_y would have pure integer values and makes them suitable for indexing the look-up table. The entries of the look-up table are pre-computed and rounded off to integer degree values. This eliminates the need for floating point calculations and entails small rounding errors. The verification process of initial seed points is described in the following steps:

Step 1. In this step, the unidirectional property of gradient vectors calculated at a seed point and its neighboring points is verified. First, the gradient vector $\overrightarrow{\nabla p^i}$ is calculated using the horizontal and vertical gradient masks (1) centered at seed point p^i. Next, the coordinates of the left and right neighboring points are identified by defining two scan lines S_L and S_R, both perpendicular to the vector $\overrightarrow{\nabla p^i}$, but in the reverse directions. The scan lines S_L and S_R are defined as set of points along the following direction vectors, respectively:

$$\overrightarrow{S_L} = [\, -\nabla_y p^i \ \ \nabla_x p^i] \tag{3-1}$$
$$\overrightarrow{S_R} = [\, \nabla_y p^i \ \ -\nabla_x p^i] \tag{3-2}$$

Starting from the seed point p^i, the angle of the gradient vector is then calculated for each point on the scan lines within a certain distance d. If the seed point and its left and right neighbors are on a locally straight vessel border, the following condition must be satisfied:

$$\forall\, m \in (S_R \cup S_L):\ \max\{|\theta_{p^i} - \theta_m|\} \le \varphi \tag{4}$$

where m is a point on either scan lines and φ is angular tolerance required to account for jagged edges and quantization effects. Ideally, an optimal value of φ must be estimated for each new frame. However, for efficiency reasons, a single value between 30° and 45°is chosen for φ which yields satisfactory results in experiments on several images. The parameter d can be used to control the strictness of the validation process and can be either 1 or 2 or more.

ISBN: 978-988-18210-4-1
ISSN: 2078-0958 (Print); ISSN: 2078-0966 (Online)

Step 2. To ensure that a seed point which is validated in the previous step is located on a boundary of a linear feature, a corresponding opposite point on the opposite boundary must be explored. By assuming the existence of two nearly parallel vessel boundaries, it is expected that the angle of the gradient vectors calculated at a seed point and its corresponding opposite point is differ by$180 \pm \varphi$. This condition is verified by employing another scan line along the opposite direction of the gradient vector $\overrightarrow{\nabla p^i}$. Let $\overrightarrow{S_O}$ denote the direction of the opposite scan line and q^i be a point on $\overrightarrow{S_O}$ within maximum expected vessel width *M*. The search for corresponding opposite point is started at point p^i and terminated if:

$$\left|180° - \left|\, \theta_{p^i} - \theta_{q^i}\right|\right| < \varphi \qquad (5)$$
$$q^i = 1,2,\ldots,M$$

with this formulation the algorithm returns the first matched point as the corresponding opposite point q^i. Otherwise, this step would fail and another seed point would be verified anew. This prevents the problem of misidentification where some vessels run close to each other.

Step 3. If the opposite point is properly selected in the previous step, the gradient vectors calculated at the opposite point and its neighbors must satisfy the conditions explained in step1.In fact, the verification of unidirectionality of gradient vectors is repeated for the opposite point q^i as described in step1.

Step 4. The previous steps can effectively verify that a given candidate seed point lies on a vessel border. However, to avoid false detections and erroneous tracing, the seed points verified in the previous steps must be validated based on their local contrast values. In this step, a seed point is considered as a valid seed point if the local contrast at the seed point is less than or equal to an adaptive contrast threshold T_c which is calculated as follows:

$$T_c = \mu_c - (\tau\,.\,\sigma_\mu) \qquad (6)$$

where μ_c is the mean contrast value of the seed points validated through steps 1-3 and σ_μ is the standard deviation calculated based on μ_c. Parameter τ is a scaling factor whose value lies between 0 and 1 and can be used to control the sensitivity of the validation algorithm to noise and contrast variations. The value of the local contrast at a given point p is denoted by C_P and is estimated by:

$$C_P = |\nabla_x p| + |\nabla_y p| \qquad (7)$$

where $\nabla_x p$ and $\nabla_y p$ are the responses of x and y gradient masks centered at point p.

The above steps are checked in the order in which they are defined and a given seed point is discarded if it fails in any one of the steps. For each validated seed point, the tracing algorithm is initiated twice, once in direction $\overrightarrow{S_L}$ and once along $\overrightarrow{S_R}$.

C. Edge based tracing

In this step, the tracing algorithm explores the boundary points using a direction vector perpendicular to $\overrightarrow{\nabla p^i}$. Starting

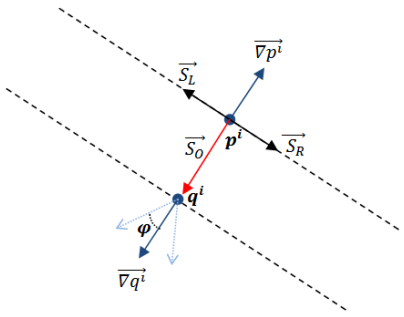

Fig. 2. Gradient vectors, scan lines, and angular tolerance for validating the seed point p^i located on a vessel boundary.

from validated seed point p^i, and the orientation of its corresponding gradient vector $\overrightarrow{\nabla p^i}$, the location of the next boundary point p^{i+1} is estimated by an extrapolation-update equation of the form:

$$\tilde{p}^{i+1} = p^i + \alpha\, \overrightarrow{\nabla p^i}\perp \qquad (8)$$

where α is a step size and $\overrightarrow{\nabla p^i}\perp$ is a direction vector perpendicular to $\overrightarrow{\nabla p^i}$. After estimating the location of the next point, Bresenham algorithm [12] is used to connect p^i and p^{i+1}.The above equation produces inaccurate traces especially when it is applied to images with low contrast or noisy images. It may be guided toward the inner part of the large vessels or background pixels. This problem can be overcome by adding an edge localization step to the tracing algorithm which is described in the next section.

D. Edge localization

In order to obtain more accurate tracing results, the edge localization step explores the strongest edge point near the estimated point $\tilde{p}^{i+1}$.The purpose of this step is to adjust the location of the next boundary point p^{i+1} by examining its neighboring points along $\overrightarrow{\nabla p^i}$ and $\overrightarrow{-\nabla p^i}$. Starting from the estimated point $\tilde{p}^{i+1}$, two scan lines are established along $\overrightarrow{\nabla p^i}$ and $\overrightarrow{-\nabla p^i}$ each within a small length r:

$$r = 2 + \lceil(\tan\varphi)\,.\,\alpha\rceil \qquad (9)$$

where the constant value 2 is needed to calculate the kernel response at first two points of each scan line.

The points on the scan lines are connected sequentially to form a sequence of gray-level values. The precise location of the next point p^{i+1} is then determined by exploring a point with maximum absolute response value of the 1-D edge kernel $[1,2,0,-2,-1]^T$ over the sequence. This correction process improves the accuracy of the tracing algorithm in terms of estimating the true location of the boundary points.

E. Stopping conditions

The tracing algorithms stops tracing if one or more of the following conditions are satisfied: 1) the new point lies outside the image field; 2) a previously detected boundary intersects the current one and 3) the sum of absolute values of the gradient components calculated at point p^{i+1} is below the sensitivity threshold T_c (described in step 4 of the seed point validation algorithm). The value of this threshold can be

ISBN: 978-988-18210-4-1
ISSN: 2078-0958 (Print); ISSN: 2078-0966 (Online)

adjusted by parameter τ in (6). Low values of this threshold make the tracing algorithm more sensitive to small contrast variations around the vessel boundaries and results in more background traces. High values of the threshold result in early stopping and create premature traces especially in low contrast frames.

III. Results and Discussion

We applied our algorithm to five digital X-ray angiograms acquired with a GE-Innova 2100^{IQ} system. Figures 3(b), 3(d) and 3(f) show example results of using our algorithm for extracting the boundaries of the vessels in figures 3(a), 3(c) and 3(e). The image has spatial resolution of 512*512 and 8-bit quantization and the parameters were set to the following values: (1) number of grid lines N=12 (2) neighborhood size N_s=30; (3) maximum expected vessel width M=25; (4) angular tolerance φ=30°; (5) verification distance d=3; (6) contrast sensitivity control parameter τ=0.50.

To show the effectiveness of our method, we compared the running time of our seed point selection and validation algorithms with the same steps in a kernel based method proposed by Can et al. [8]. Table I shows the running time comparison on different number of predefined seed points. The computer used is a 2.4Ghz CPU Intel Pentium 4 running Windows XP.

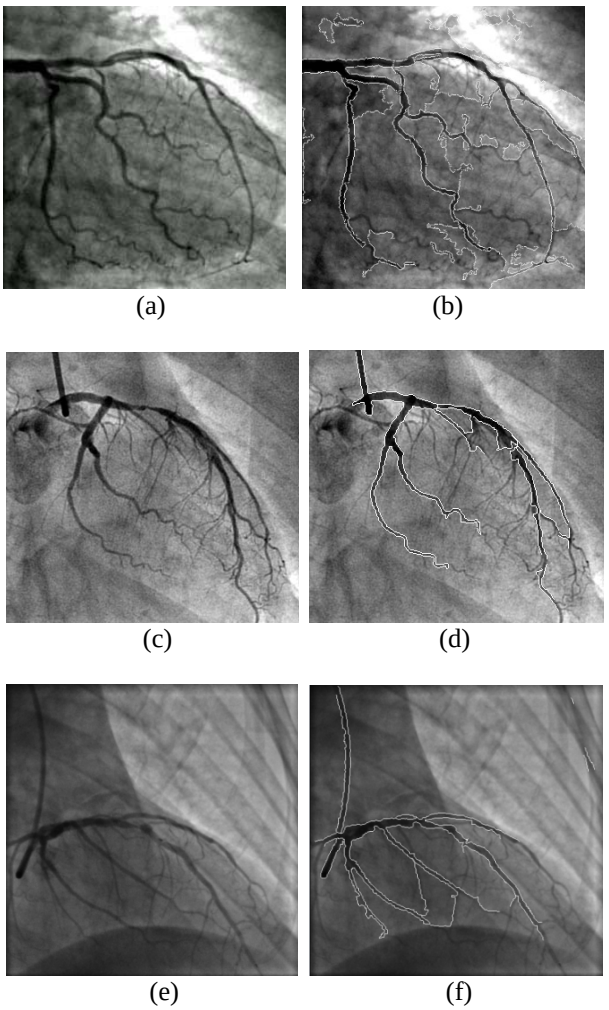

Fig. 3. Examples of vessel boundary detection. (a), (c) and (e) input images. (b), (d) and (f) results of applying our algorithm.

Table I. Running times of the seed point selection and validation steps in Can et al. and our algorithm.

No. of Seed points	Running Times (ms)	
	Can et al.	Our algorithm
100	393	124
200	740	230
300	1257	389
400	1673	514
500	1995	607

The output results illustrate that the method is able to differentiate vessel structures from background and non-vessel objects. Furthermore, to a large extent, the algorithm is able to detect the vessel boundaries and terminate rapidly for the false detections. However, some undetected vessel branches and background traces exist. This is mainly due to low signal to noise ratio and contrast variations in the image. The running time results show that our new seed point validation algorithm is about 3 times faster than kernel based algorithms. Its prominency comes from avoiding exhaustive vessel direction estimation using 2-D differentiator kernels and angular quantization error associated with previous methods [8]-[11].

IV. Conclusions and Future Works

In this paper, a new vessel tracing algorithm for detecting the feature boundaries of the vessels in live angiogram sequences is presented. Without any preprocessing steps, the algorithm merely processes a minimal fraction of pixels which are located on the vessel boundaries and directly traces the boundary points using an efficient gradient-based update equation. Clearly, the results show that vessel boundary segmentation can be obtained without requiring exhaustive directional searches initiated at each centreline point. Furthermore, centerline representation can be achieved by exploiting the precise location of the extracted left and right boundary points. The comparison results illustrate that the method is very fast compared with other methods in the literature. Our future plan is to improve the accuracy of our algorithm concerning its ability in preventing false traces and detecting more vessel segments. We also plan to develop a more robust stopping criterion, possibly by incorporating local history of the current trace and signal-to-noise ratio analysis.

References

[1] M. Sonka, M. D. Winniford, and S. M. Collins, "Robust simultaneous detection of coronary borders in complex images," IEEE transactions on medical imaging, vol. 14, pp. 151-161, 1995.

[2] J. Staal, M. D. Abràmoff, M. Niemeijer, M. A. Viergever, and B. van Ginneken, "Ridge-based vessel segmentation in color images of the retina," IEEE Transactions on Medical Imaging, vol. 23, pp. 501-509, 2004.

[3] F. Zana and J. C. Klein, "Segmentation of vessel-like patterns using mathematical morphologyand curvature evaluation," IEEE Transactions on Image Processing, vol. 10, pp. 1010-1019, 2001.

[4] F. K. H. Quek and C. Kirbas, "Vessel extraction in medical images by wave-propagation and traceback," IEEE transactions on Medical Imaging, vol. 20, pp. 117-131, 2001.

ISBN: 978-988-18210-4-1
ISSN: 2078-0958 (Print); ISSN: 2078-0966 (Online)

[5] A. Vasilevskiy and K. Siddiqi, "Flux maximizing geometric flows," IEEE Transactions on Pattern Analysis and Machine Intelligence, pp. 1565-1578, 2002.
[6] R. Collorec and J. L. Coatrieux, "Vectorial tracking and directed contour finder for vascular network in digital subtraction angiography," Pattern recognition letters, vol. 8, pp. 353-358, 1988.
[7] Y. Sun, "Automated identification of vessel contours in coronaryarteriograms by an adaptive tracking algorithm," IEEE transactions on medical imaging, vol. 8, pp. 78-88, 1989.
[8] A. Can, H. Shen, J. N. Turner, H. L. Tanenbaum, and B. Roysam, "Rapid automated tracing and feature extraction from retinal fundus images using direct exploratory algorithms," IEEE Transactions on Information Technology in Biomedicine, vol. 3, pp. 125-138, 1999.
[9] K. A. Al-Kofahi, S. Lasek, D. H. Szarowski, C. J. Pace, G. Nagy, J. N. Turner, and B. Roysam, "Rapid automated three-dimensional tracing of neurons from confocal image stacks," IEEE Transactions on Information Technology in Biomedicine, vol. 6, pp. 171-187, 2002.
[10] K. A. Al-Kofahi, A. Can, S. Lasek, D. H. Szarowski, N. Dowell-Mesfin, W. Shain, J. N. Turner, and B. Roysam, "Median-based robust algorithms for tracing neurons from noisy confocal microscope images," IEEE Transactions on information technology in biomedicine, vol. 7, pp. 302-317, 2003.
[11] Y. Zhang, X. Zhou, A. Degterev, M. Lipinski, D. Adjeroh, J. Yuan, and S. T. C. Wong, "A novel tracing algorithm for high throughput imaging Screening of neuron-based assays," Journal of neuroscience methods, vol. 160, pp. 149-162, 2007.
[12] J. E. Bresenham, "Algorithm for computer control of a digital plotter," IBM Syst J vol. 4, pp. 25–30, 1965.

ISBN: 978-988-18210-4-1
ISSN: 2078-0958 (Print); ISSN: 2078-0966 (Online)